Tribology International 86 (2015) 1–9

Contents lists available at ScienceDirect

Tribology International

journal homepage: www.elsevier.com/locate/triboint

Film thickness and traction curves of wind turbine gear oils

Carlos M.C.G. Fernandes [a,*], Pedro M.T. Marques [a], Ramiro C. Martins [a], Jorge H.O. Seabra [b]

[a] INEGI, Universidade do Porto, Campus FEUP, Rua Dr. Roberto Frias 400, 4200-465 Porto, Portugal
[b] FEUP, Universidade do Porto, Rua Dr. Roberto Frias s/n, 4200-465 Porto, Portugal

ARTICLE INFO

Article history:
Received 4 December 2014
Received in revised form
6 January 2015
Accepted 17 January 2015
Available online 24 January 2015

Keywords:
Wind turbine gear oils
Film thickness
Coefficient of friction
Stribeck curve

ABSTRACT

The film thickness and the traction curves of four fully formulated wind turbine gear oils were measured on a ball-on-disc device. All oils have the same viscosity grade (ISO VG 320) and different formulations: ester, mineral, PAO and mineral+PAMA.

Film thickness and traction coefficient results will be presented. The film thickness measurements were compared with predictions using film thickness equations from the literature.

1. Introduction

The prediction of film thickness and traction coefficient in concentrated EHL line and point contacts that can be found in mechanical components such as gears, cams and rolling bearings [1] is of major interest.

In the 1960s Dowson and Higginson [2] performed a series of numerical simulations assuming isothermal Newtonian fluid model and exponential piezo-viscosity to develop the most popular minimum film thickness formula to EHL line contacts.

The traction coefficient can be characterized by the low shear viscosity, limiting shear modulus, and the limiting shear stress the lubricant can withstand. Understanding the traction properties is of great interest in the development of lubricants or conversely for a proper choice of a lubricant for a given application [3,4].

The generation of electricity by wind power is becoming very important due to the concerns about the effects of global warming [5,6]. To make wind energy competitive with other power plants in the near future, enhancements on availability, reliability and lifetime of the wind turbines will be required [7–10]. For this particular case, the wind turbine gearbox problems can start with the oil that should be treated with caution as a mechanical component. According to DIN recommendations the best viscosity and anti-scuffing properties are reached for oil operating temperatures above 80 °C. In wind turbine gearboxes where operating temperatures sometimes do not exceed 60 °C the anti-scuffing class tends to drop, resulting in a worst start-up behaviour and higher debris level generated [11]. A major problem with this kind of application is to assure an effective lubricant film and the oil must be synthetic if the oil sump temperature is higher than 80 °C [12,13].

In the previous works, different wind turbine gear oils were submitted to rolling bearing friction torque measurements [14–17] as well as gear tests [18]. Film thickness measurements using greases were recently published by Cousseau et al. [19].

This work is intended to characterize the ability of a wind turbine gear oil to generate a lubricating film. The film thickness prediction is also discussed and related to experimental results. Traction coefficient curves as well as Stribeck curves will be presented to characterize the tribological behaviour of fully formulated wind turbine gear oils.

2. Wind turbine gear oils

In order to analyse the different gear oils suitable for the lubrication of wind turbine gearboxes, four fully formulated ISO VG 320 gear oils were selected.

In between the selected gear oils, four base oils were considered:

- Mineral base oil (MINR),
- Biodegradable ester base oil (ESTR),
- Polyalphaolephin base oil with an ester compatibiliser (PAOR),
- Hydroprocessed group III base oil with a PAMA thickener (MINE).

Table 1 displays the wind turbine gear oils physical properties as well as their chemical composition. A detailed description on

* Corresponding author.
E-mail address: cfernandes@inegi.up.pt (C.M.C.G. Fernandes).

http://dx.doi.org/10.1016/j.triboint.2015.01.014
0301-679X/

Notation and units

C_0	ellipticity influence parameter (–)
COF	coefficient of friction (–)
E^*	equivalent Young Modulus (Pa)
G	material influence parameter (–)
h_0	center film thickness (m)
p_0	Hertzian contact pressure (Pa)
k	thermal conductivity (W/m K)
L^*	thermal parameter of the lubricant (–)
m	D341 viscosity parameter (–)
n	D341 viscosity parameter (–)
R_X	equivalent radius in rolling direction (m)
S_p	modified Hersey number (–)
S	Hersey number (m^{-1})
SRR	slide-to-roll ratio (%)
s	pressure–viscosity parameter (–)
t	pressure–viscosity parameter (–)
U_S	sum of the surface velocities (m/s)
U_{ball}	ball speed (m/s)
U_{disc}	disc speed (m/s)
U	speed influence parameter (–)
W	load influence parameter (–)
α	pressure–viscosity coefficient (Pa^{-1})
α_t	thermal expansion coefficient (–)
β	thermoviscosity coefficient (K^{-1})
η	dynamic viscosity (Pa s)
ϕ_T	thermal reduction factor (–)
ν	kinematic viscosity (cSt)
ρ	density (g/cm^3)
θ_{oil}	oil bath temperature (°C)
Λ	specific film thickness (–)

the physical properties can be found in the previous works with same oils [14–18].

The FTIR analysis was used in order to identify some of the characteristic peaks of the lubricants (see Fig. 1).

3. Film thickness

3.1. Materials and methods

Film thickness measurements were performed on an EHD2 ball-on-disc test apparatus from PCS Instruments equipped with optical interferometry as presented in Fig. 2. The machine measures the lubricant film thickness properties in the contact formed between a 3/4 in diameter steel ball and a rotating glass disk by optical interferometry. The lubricant film thickness at any point in the image can be accurately calculated by measuring the wavelength of light at that point. Normally the system measures the wavelength of the light returned from the central plateau of the contact and hence calculates the central film thickness.

Optical interferometry measurements of lubricant film thickness have already been described by several authors. Details of this technique have been reported elsewhere [20–22] and only a brief description will be given here.

The lubricated contact is formed by the reflective steel ball and the flat surface of the glass disc. The glass disc is coated with a semi-reflecting chromium coating on top of which a spacer layer of SiO_2 is deposited. The load is applied by moving the ball upwards toward the disc. The disc is mounted on a shaft driven by an electric motor. The steel ball is also controlled by an electric motor, making it possible to run the tests under rolling/sliding conditions.

The EHD2 method to perform film thickness measurements is described in 4 steps (see Fig. 3):

1. The contact is illuminated by a white light source directed down a microscope through a glass disc on to the contact.
2. Part of the light is reflected from the Cr layer and part travels through the SiO_2 layer and fluid film and is reflected back from the steel ball.
3. Recombining the two light paths forms an interference image which is passed into a spectrometer and high resolution black and white CCD camera.
4. The camera image is captured by a video frame grabber and analysed by the control software to determine the film thickness.

The method used for translating the optical phase difference map into film thickness has been described by several authors [22–24].

Table 1
Physical and chemical properties of wind turbine gear oils used.

Parameter Base oil	Unit [–]	MINR Mineral	ESTR Ester	PAOR Polialphaolefin	MINE Mineral+PAMA
Chemical composition					
Zinc (Zn)	[ppm]	0.9	6.6	3.5	< 1
Magnesium (Mg)	[ppm]	0.9	1.3	0.5	< 1
Posphorus (P)	[ppm]	354.3	226.2	415.9	460
Calcium (Ca)	[ppm]	2.5	14.4	0.5	2
Boron (B)	[ppm]	22.3	1.7	28.4	36
Sulphur (S)	[ppm]	11,200	406	5020	6750
Physical properties					
Density at 15 °C	[g/cm^3]	0.902	0.915	0.859	0.893
Thermal expansion coefficient ($\alpha_t \times 10^4$)	[–]	−5.8	−8.1	−5.5	−6.7
Viscosity at 40 °C	[cSt]	319.22	302.86	313.52	328.30
Viscosity at 70 °C	[cSt]	65.81	77.48	84.99	93.19
Viscosity at 100 °C	[cSt]	22.33	34.85	33.33	37.13
m	[–]	9.066	7.582	7.351	7.048
n	[–]	3.473	2.880	2.787	2.663
Thermoviscosity at 40 °C ($\beta \times 10^{-3}$)	[K^{-1}]	63.88	49.09	50.68	49.33
Thermoviscosity at 70 °C ($\beta \times 10^{-3}$)	[K^{-1}]	42.83	35.25	36.16	35.48
Thermoviscosity at 100 °C ($\beta \times 10^{-3}$)	[K^{-1}]	30.07	26.19	26.72	26.40
VI	[–]	85	140	150	163

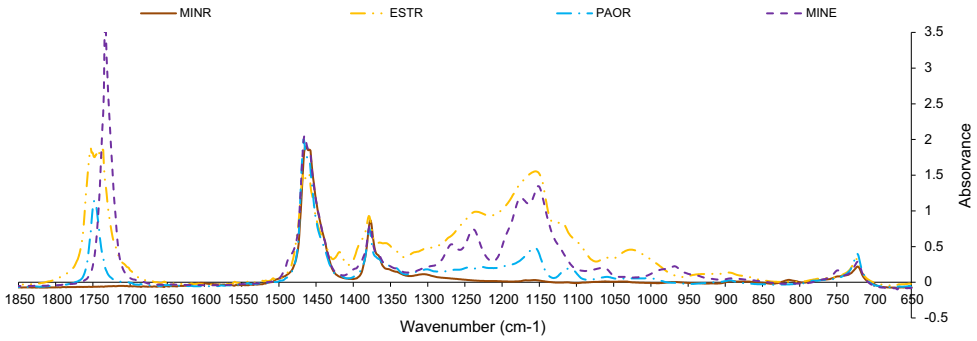

Fig. 1. IR spectrum.

Fig. 2. EHD2 ball-on-disc test apparatus from PCS instruments.

3.2. Test specimens

The standard ball specimen has a 3/4 in (19.05 mm) diameter and is made from carbon chrome steel and has a high grade surface finish to ensure good reflectivity. The roughness of the ball and disc are presented in Table 2 according to information provided by the manufacturer.

The discs were made of glass coated with approximately 20 nm of chromium and 500 nm of silica. The disc supports a maximum Hertz pressure of approximately 0.7 GPa. The silica spacer layer has a refractive index of 1.4785 according to the manufacturer.

The physical properties of the lubricants are presented in Table 1 and the ball and disc properties are presented in Table 2.

3.3. Test procedures

A set of lubricant film thickness measurements were carried out under fully flooded lubrication for all wind turbine gear oils presented in Section 2.

The load applied was 50 N, which corresponds to a maximum Hertz pressure of $p_0 = 0.66$ GPa. Three operating temperatures were used: 50, 80 and 100 °C. The tests were carried out with a 3% slide-to-roll ratio (*SRR*), defined by the following equation:

$$\text{SRR}\ [\%] = 2 \times \frac{(U_{disc} - U_{ball})}{(U_{disc} + U_{ball})} \times 100 \quad (1)$$

The entrainment speed range was different for each operating temperature. The highest entrainment speed is always the same and equal to 2 m/s. The lowest value is 0.1 m/s for 50 °C; 0.25 m/s for 80 °C and 0.5 m/s for 100 °C. These conditions assure a measured film thickness not lower than 100 nm, thus ensuring that ball-disc contact does not occur. The highest entrainment speed was limited because the maximum measurement range of the optical device is around 1000 nm.

The lubricant was heated in the container where the ball is partially submerged (up to the centre of the ball). The container which supplies the contact stored up to 120 ml of oil. The oil tests carried out with this configuration presented a slightly temperature deviation of ± 1.0 °C. The temperature is measured in the oil sump.

The temperature oscillations were considered when calculating all the parameters presented ahead. For each operating temperature, the film thickness was measured from the highest to the lowest entrainment speed, and then a new measurement was done in the opposite direction (from lowest up to the highest entrainment speed). This procedure allows to verify the repeatability of the measurements which was very good.

3.4. Experimental results

The lubricant parameter (*LP*) defined by the product $\text{LP} = \eta \times \alpha$, was calculated using the pressure–viscosity Eq. (2). The corresponding values for all wind turbine gear oils and for the temperatures of 50, 80 and 100 °C are shown in Table 3. At constant temperature the *LP* values for the different lubricants are very similar.

$$\alpha = s \cdot \nu^t \times 10^{-8} \quad (2)$$

Fig. 4 shows the film thickness measurements for a wide range of the entrainment speed and for the temperatures of 50, 80 and 100 °C, for the selected wind turbine gear oils.

Whatever the temperature considered, the film thickness measurements for oils MINR, ESTR and PAOR are always very similar, as presented in Fig. 4. This is not surprising since for the same temperature these oils have almost the same *LP* values.

The film thickness of PAOR is about 6% higher than ESTR, which is approximately the same difference found on the LP. In fact, the measurements follow the behaviour of the *LP* parameter, since for same conditions of speed and geometry, only the dynamic viscosity and the pressure–viscosity (*LP*) play a role on film thickness.

The MINE oil has higher *LP* parameter than PAOR and ESTR at 50 and 80 °C, but presented lower film thickness which can be related with shear thinning effects. The viscosity of a mineral oil with 4% of PAMA was measured and a non-Newtonian behaviour was observed when the shear rate increases, resulting in shear thinning effect [25]. A similar behaviour is expected for a mineral oil with a much higher PAMA content, like MINE.

For all operating temperatures tested, both ESTR and PAOR show similar behaviour. MINE and MINR become close when temperature rises.

3.5. Film thickness prediction

In a recent study, Van Leeuwen [26] demonstrated that the centre film thickness values predicted by the equations proposed by Chittenden et al. [27] and by Hamrock et al. [28] correlated very

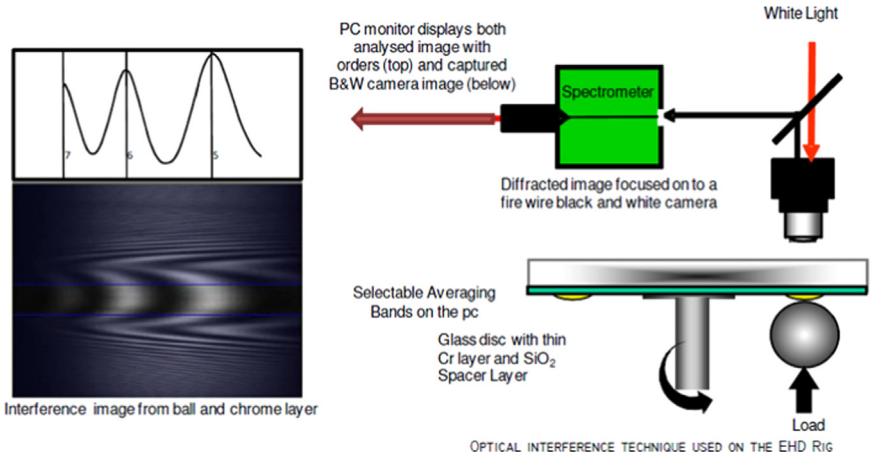

Fig. 3. Optical interference technique used in EHD2 test rig.

Table 2
Ball and disc data.

Property	Ball	Disc
Elastic modulus – E [GPa]	210	64
Poisson coefficient – ν [–]	0.29	0.2
Radius – R (mm)	19.05	50
Surface roughness – Ra (nm)	20	≈ 5
Spacer layer thickness – (nm)	–	≈ 500
Spacer layer refractive index – (–)	–	≈ 1.4785

Table 3
Lubricant parameter ($LP \times 10^{10}$) for the wind turbine gear oils tested.

θ_{oil}	MINR	ESTR	PAOR	MINE
50 °C	32.03	23.30	24.79	25.28
80 °C	6.65	6.52	6.72	6.73
100 °C	3.08	3.38	3.44	3.40

well ($R^2 > 97\%$) with accurate film thickness measurements for the same operating conditions and for a lubricant with a known pressure–viscosity coefficient (α).

The equations proposed by Chittenden et al. and Hamrock et al. use the Roelands equation [29] to describe viscosity dependence on pressure and on temperature and take into account fluid compressibility according to Dowson and Higginson [2].

Based on the evidence reported by Van Leeuwen [26], Eq. (3) proposed by Hamrock and Dowson [30] will be used in this work to predict the centre film thickness in point contacts:

$$h_0 = 2.69 \cdot R_X \cdot U^{0,67} \cdot G^{0,53} \cdot W^{-0,067} \cdot C_0 \tag{3}$$

with

$$U = \frac{\eta_0 \cdot U_S}{E^* \cdot R_X} \tag{4}$$

$$G = \alpha \cdot E^* \tag{5}$$

$$W = \frac{F_n}{E^* \cdot R_X^2} \tag{6}$$

The corrected equation taking into account the inlet shear heating of the lubricant and the corresponding thermal correction (ϕ_T) is presented in the following equation:

$$h_{0C} = \phi_T \cdot h_0 \tag{7}$$

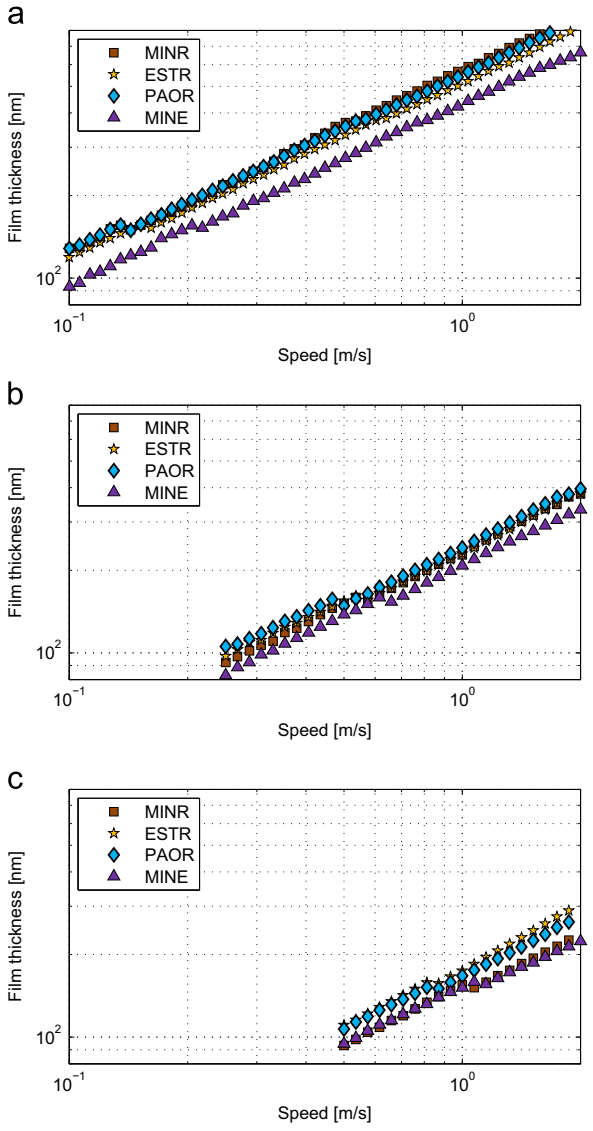

Fig. 4. Film thickness measurements for different wind turbine gear oils. (a) 50 °C, (b) 80 °C and (c) 100 °C.

Thermal correction ϕ_T used was proposed by Gupta et al. [31], as shown in the following equations:

$$\phi_T = \frac{1 - 13.2 \cdot (p_0/E^*) \cdot (L^*)^{0.42}}{1 + 0.213(1 + 2.23 \cdot S^{0.83}) \cdot (L^*)^{0.64}} \tag{8}$$

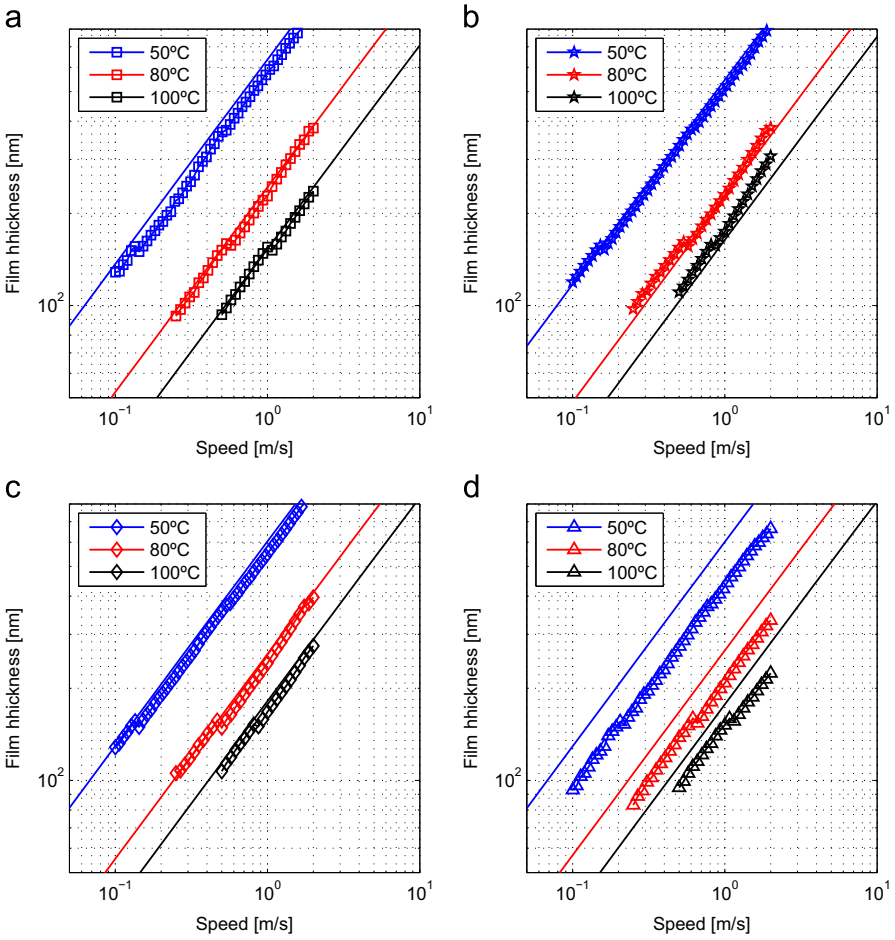

Fig. 5. Film thickness measurements vs predictions for different wind turbine gear oils. (a) MINR, (b) ESTR, (c) PAOR and (d) MINE.

$$L^* = \frac{\beta_L \cdot \eta \cdot U_S}{k_L} \tag{9}$$

Fig. 5 presents film thickness predicted by Eqs. (3)–(9) – straight lines and the corresponding experimental measurements – markers, for all gear oils and operating temperatures considered. The correlation between predicted and experimental values is very good for gear oils MINR, PAOR, and ESTR, whatever the entrainment speed and operating temperature. However, such good correlation is not observed in the case of MINE gear oil. In fact, it has been reported in the literature [25] that mixtures of mineral or synthetic base oils with polymers, such as gear oil MINE, exhibit a clear non-Newotonian and shear-thinning behaviour. In this case, the film thickness predictions overestimate the film thickness measurements.

The difference between predicted and measured centre film thickness values might be minimized if the pressure–viscosity coefficient is minimized.

The film thickness for all the oils follows the usual trend of the dimensionless velocity group (U) [2], the rate is $h_{0C} \propto U^{0.67}$.

3.6. Pressure–viscosity

The difference between the predicted and the measured centre film thickness values might be minimized if the pressure–viscosity coefficient is optimized. A bounded non-linear least squares optimization algorithm was used to calculate the pressure–viscosity coefficient that is most compatible with film thickness measurements. The objective function is the relative difference between the experimental and numerical data. Table 4 shows the pressure–viscosity coefficients given by Gold's equation [32], α_{Gold}, as well as those resulting the minimization process mentioned above, α_{FTM}.

Table 4
Pressure–viscosity coefficients determined based on film thickness measurements (α_{FTM}) and Gold equation (α_{Gold}).

θ_{oil}	Pressure–viscosity	MINR	ESTR	PAOR	MINE
50 °C	α_{FTM}	1.443	1.092	1.143	0.651
	α_{Gold}	1.995	1.329	1.469	1.346
80 °C	α_{FTM}	1.403	1.038	1.053	0.653
	α_{Gold}	1.667	1.131	1.262	1.112
100 °C	α_{FTM}	1.308	1.139	0.942	0.644
	α_{Gold}	1.526	1.064	1.181	1.011

The values given by Gold's equation are clearly dependent on the lubricant formulation and on the temperature. The α_{FTM} values are, in general, smaller than the corresponding α_{Gold} values, and such difference is very large in the case of the MINE gear oil (42% lower). The influence of the temperature also does not seem consistent, e.g. $\alpha_{FTM,}$ at 100 °C > α_{FTM} at 80 °C for ESTR and α_{FTM} at 40 °C ≈ α_{FTM} at 80 °C for MINR.

This indirect prediction of the pressure–viscosity coefficient using film thickness measurements, although very useful, needs further research and these is not a clear consensus in the literature [33,34].

4. Traction and stribeck curves

4.1. Materials and methods

Wind turbine gear oils traction coefficient measurements were performed on an EHD2 ball-on-disc device from PCS Instruments, under controlled temperature. This device was described in the previous section.

For the traction measurements the ball runs against a steel disc and the load is applied by moving the ball upwards towards disc, generating contact pressures up to 1.11 GPa. The remaining conditions related to machine operation capabilities were described in Section 3.1.

4.2. Test specimens

The ball and disc used were made from carbon chrome steel, with 3/4 in (19.05 mm) and 100 mm diameters, respectively. The ball and disc roughness was provided by the manufacturer. The ball and disc properties are presented in Table 5 and the oil physical properties are presented in Table 1.

Table 5
Ball and disc data.

Property	Ball	Disc
Elastic modulus $-E$ (GPa)	210	210
Poisson coefficient $-\nu$ (–)	0.29	0.29
Radius $-R$ (mm)	19.05	50
Surface roughness $-\sigma$ (μm)	0.02	0.20

4.3. Test procedure

A set of tests were carried out to measure the traction coefficient of the wind turbine gear oils presented in Section 2.

The load applied was 50 N, which corresponds to a maximum Hertz pressure of $p_0 = 1.11$ GPa. Three operating temperatures were used: 50, 80 and 100 °C. The slide-to-roll ratio was varied from 1 to 50% for three different entrainment speeds of 0.5, 1 and 2 m/s. In all cases the disc rotated faster than the ball. The temperature control is described in Section 3.3.

The test cycle contained several loops where the entrainment speed was kept constant while the *SRR* was increased from 1 to 50% and then decrease up to 1% again. The entrainment speed was held at 2 m/s in the first loop and decreased in each loop down to 0.5 m/s.

For the Stribeck curves experiments, the SRR was kept constant with the value of 25% and the speed was changed between 0.01 m/s and 3 m/s. It used two different operating temperatures: 80 °C and 120 °C. The higher value of temperature was used to achieve boundary film lubrication conditions.

4.4. Traction coefficient

The traction coefficient results are presented in Fig. 6. The relative performance of the oils is almost independent of the

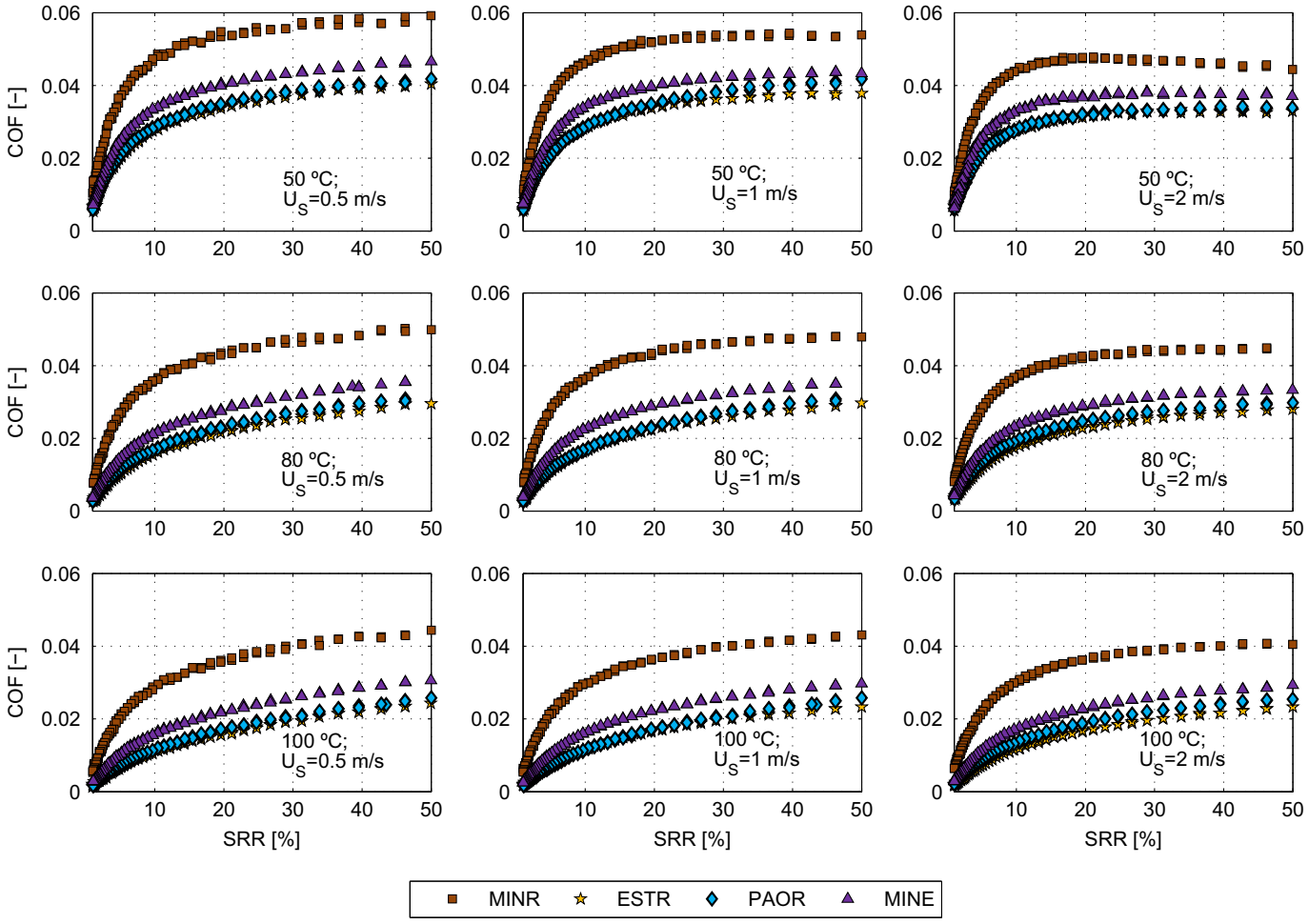

Fig. 6. Traction coefficient measurements for different wind turbine gear oils.

temperature and entrainment speed, and MINR always generates the highest traction coefficient, followed by MINE and PAOR and ESTR have similar behaviour (MINR > MINE > PAOR ≈ ESTR).

To understand the lubrication regime that occurs for each test performed, the specific film thickness was calculated for each operating temperature and the results are presented in Fig. 7. The results show that above 1 m/s at 50 °C the tests were performed under full film conditions ($\Lambda > 2$) no matter the oil. It can be observed that for all lubricating oils, the increase of temperature decreases the coefficient of friction. Such behaviour is expected for full film lubrication conditions, as suggested in the literature [35].

The coefficient of friction is reduced for all lubricating oils when the speed increases. However the oil that appears to be most influenced by the speed is the MINR which has the lowest viscosity index.

The results suggest that the nature of the oil, i.e. base oil, clearly defines the friction behaviour of the oils. The oils are fully formulated. However, MINR traction coefficient is higher than the other oils. So, the base oil is the most important factor for the traction coefficient [35].

4.5. Stribeck curve

The Stribeck curves were measured at 80 and 120 °C and are presented in Fig. 8. The coefficients of friction are presented using the modified Hersey number suggested by Brandão [35] and given by Eq. (10). The original Hersey number (S) is given by Eq. (11):

$$S_p = \frac{\eta \cdot U_S \cdot \alpha^{1/2}}{F^{1/2}} \tag{10}$$

$$S = \frac{\eta \cdot U_S}{F} \tag{11}$$

Brandão proposed that for a modified Hersey number $S_p < 10^{-9}$, the contact is under boundary film lubrication, while for $S_p > 10^{-7}$ it is under full film lubrication.

The results presented in Fig. 8 show the expected behaviour for $S_p > 10^{-7}$. Under these conditions the coefficient of friction of the synthetic formulations is very similar for the same temperature and significantly lower than MINR. The influence of the temperature is clear for all the wind turbine gear oils: the coefficient of friction decreases when the temperature increases (see Fig. 8 (a) and (b)).

At 80 °C, the modified Hersey number never reaches 10^{-9} and so the oils remain under mixed film lubrication for values $S_p < 10^{-7}$.

At 120 °C the oils come closer to the expected boundary lubrication condition, and for these conditions the oils show very similar coefficients of friction, see Fig. 8(b), whatever the base oil and additive package considered.

For a modified Hersey number $S_p \approx 10^{-6}$, the oils show the following behaviour: $\mu_{EHD}^{MINR} > \mu_{EHD}^{MINE} > \mu_{EHD}^{PAOR} > \mu_{EHD}^{ESTR}$.

According to Brandão et al. [35], the limiting shear stress and Lubricant Parameter (LP) of mineral oils are higher than any other oil formulation studied in his work. Additionally, Brandão also showed that for the same operating condition the lubricant with highest Lubricant Parameter (LP) and limiting shear stress, in our study MINR, promotes the highest coefficient of friction. It was then concluded that the base oil is the most important factor for the friction properties under full film conditions.

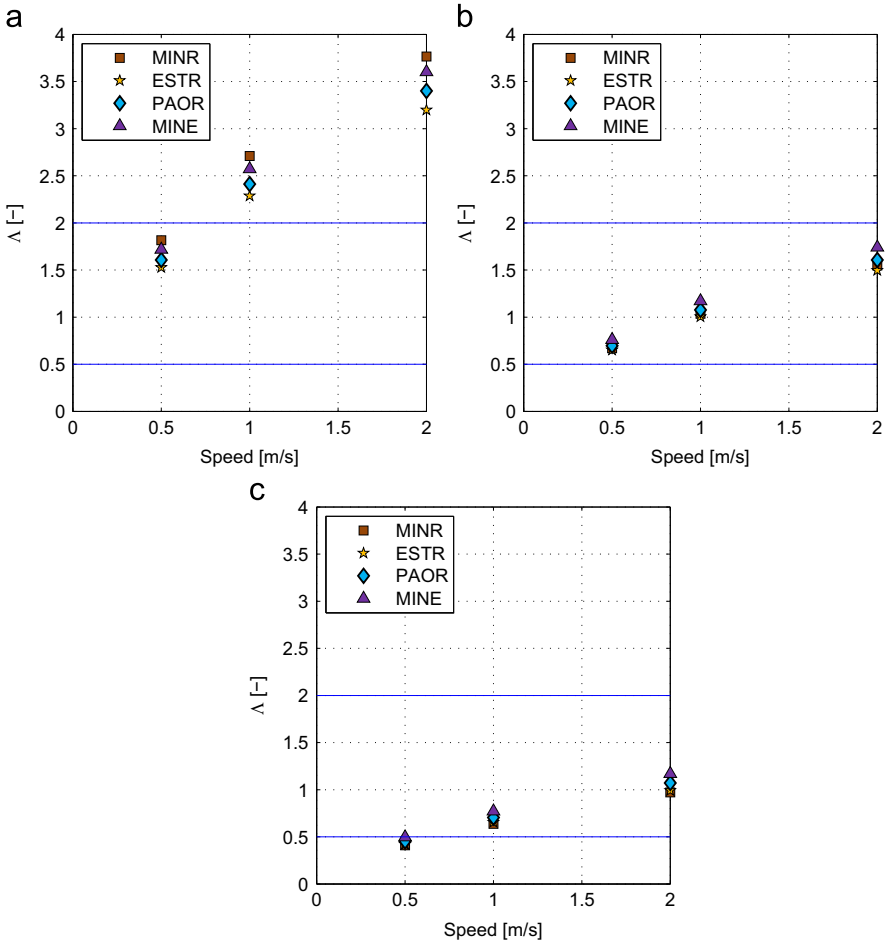

Fig. 7. Specific film thickness predictions for the traction coefficient measurements. (a) 50 °C, (b) 80 °C and (c) 100 °C.

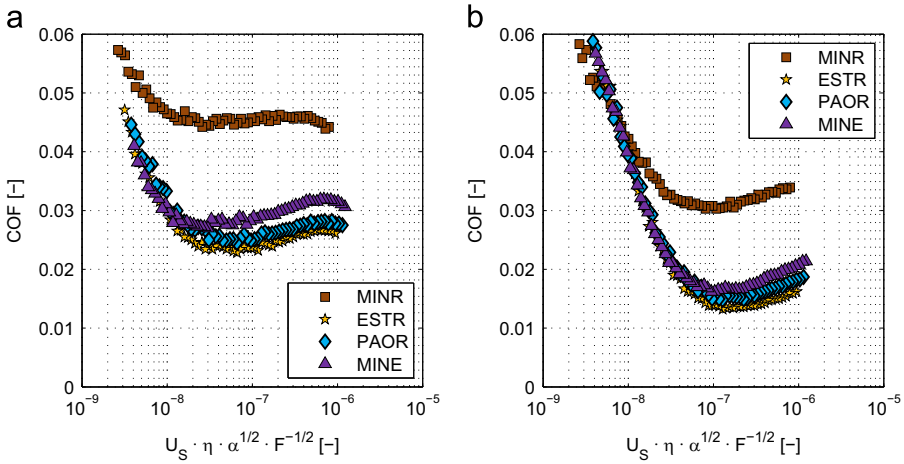

Fig. 8. Stribeck curve measurements. (a) 80 °C and (b) 120 °C.

5. Conclusion

The film thickness and the traction coefficient were measured for four different wind turbine gear oil formulations, on a ball-on-disc apparatus.

The film thickness tests clearly show that no substantial differences were found between oils. The MINR oil can generate a lubricating film similar to ESTR and PAOR. MINE shows a shear thinning effect and consequently lower film thickness. This behaviour was not expected from the measured properties of MINE.

The traction coefficient tests, performed under full film conditions, allow to understand that the base oil is very important for the friction behaviour of a gear oil under these lubrication conditions. We can observe that a mineral base oil has higher friction coefficient (μ_{EHD}) than a synthetic oil or than a mineral with a viscosity modifier additive in large concentration, as the case of MINE oil. The friction behaviour of the PAO (PAOR) and of the ester (ESTR) are very similar, which has already been reported by Brandão [35]. The traction coefficient decreases with the increasing temperature and decreases with the increasing speed which is coherent with the literature [35].

The Stribeck curves show that the full film coefficient of friction is dependent on the oil formulation and large differences between MINR oil and other formulations were found. However, when the lubrication regime moves towards boundary film lubrication the coefficients of friction are similar at 120 °C for all oil formulations.

Acknowledgements

The authors acknowledge to “Fundação para a Ciência e Tecnologia” for the financial support given through the project with research contract EXCL/EMS-PRO/0103/2012.

References

[1] Anuradha P, Kumar P. New film thickness formula for shear thinning fluids in thin film elastohydrodynamic lubrication line contacts. Proc Inst Mech Eng, Part J: J Eng Tribol 2011;225(4):173–9. http://dx.doi.org/10.1177/1350650111399520 arXiv:http://pij.sagepub.com/content/225/4/173.full.pdf+html, ⟨http://pij.sagepub.com/content/225/4/173.abstract⟩.
[2] Dowson D, Higginson G. Elasto-hydrodynamic lubrication: the fundamentals of roller and gear lubrication, The commonwealth and international library. Pergamon Press; 1966 URL: ⟨http://books.google.pt/books?id=HuMuAAAAIAAJ⟩.
[3] Jost HP. Lubrication tribology – education and research. Technical report. Department of Education and Science, HMSO, London; 1966.
[4] Fang N, Chang L, Webster M, Jackson A. A non-averaging method of determining the rheological properties of traction fluids. Tribol Int 2000;33 (11):751–60. http://dx.doi.org/10.1016/S0301-679X(00)00116-X URL ⟨http://www.sciencedirect.com/science/article/pii/S0301679X0000116X⟩.
[5] High efficiency planetary gearboxes for eco-power, World Pumps 2001; (419): 34–36, http://dx.doi.org/10.1016/S0262-1762(01)80327-8.
[6] Agency EE. Europe's onshore and offshore wind energy potential – an assessment of environmental and economic constraints. EEA Technical report No 6; 2009. p. 91.
[7] McNiff B, Musial W, Errichello R. Variations in gear fatigue life for different wind turbine braking strategies, prepared for AWEA Wind Power '90, Washington, DC; 24–8 September 1990 (1991) Medium: ED. 10 p.
[8] Winkelmann L. Surface roughness and micropitting. In: National renewable energy laboratory wind turbine tribology seminar; 2011.
[9] McDade M. Gearbox reliability collaborative (grc) failure database. In: National renewable energy laboratory wind turbine tribology seminar; 2011.
[10] Jungk M. Update on the development of a full life wind turbine gear box lubricating fluid. In: National renewable energy laboratory wind turbine tribology seminar; 2011.
[11] Zellmann J. Main types of damage to wind turbine gearboxes. Wind Kraft J 2009;3:2–5.
[12] Muller J, Errichello R. Oil cleanliness in wind turbine gearboxes, Machinery lubrication; July 2002.
[13] Mitchell F. Choosing the right wind turbine lubricant. Power engineering; April 2009.
[14] Fernandes CM, Martins RC, Seabra JH. Friction torque of thrust ball bearings lubricated with wind turbine gear oils. Tribol Int 2013;58(0):47–54. http://dx.doi.org/10.1016/j.triboint.2012.09.005 URL: ⟨http://www.sciencedirect.com/science/article/pii/S0301679X12003015⟩.
[15] Fernandes CM, Martins RC, Seabra JH. Friction torque of cylindrical roller thrust bearings lubricated with wind turbine gear oils. Tribol Int 2013;59 (0):121–8 doi:http://dx.doi.org/10.1016/j.triboint.2012.05.030, URL ⟨http://www.sciencedirect.com/science/article/pii/S0301679X12001922⟩.
[16] Fernandes CM, Amaro PM, Martins RC, Seabra JH. Torque loss in thrust ball bearings lubricated with wind turbine gear oils at constant temperature. Tribol Int 2013;66(0):194–202 doi:http://dx.doi.org/10.1016/j.triboint.2013.05.002, URL: ⟨http://www.sciencedirect.com/science/article/pii/S0301679X13002041⟩.
[17] Fernandes CM, Amaro PM, Martins RC, Seabra JH. Torque loss in cylindrical roller thrust bearings lubricated with wind turbine gear oils at constant temperature. Tribol Int 2013;67(0):72–80 doi:http://dx.doi.org/10.1016/j.triboint.2013.06.016, URL: ⟨http://www.sciencedirect.com/science/article/pii/S0301679X13002363⟩.
[18] Fernandes CM, Martins RC, Seabra JH. Torque loss of type {C40} {FZG} gears lubricated with wind turbine gear oils. Tribol Int 2014;70(0):83–93 doi:http://dx.doi.org/10.1016/j.triboint.2013.10.003, URL: ⟨http://www.sciencedirect.com/science/article/pii/S0301679X13003381⟩.
[19] Cousseau T, Bjrling M, Graa B, Campos A, Seabra J, Larsson R. Film thickness in a ball-on-disc contact lubricated with greases, bleed oils and base oils. Tribol Int 2012;53(0):53–60 doi:http://dx.doi.org/10.1016/j.triboint.2012.04.018, URL: ⟨http://www.sciencedirect.com/science/article/pii/S0301679X12001429⟩.
[20] Johnston GJ, Wayte R, Spikes HA. The measurement and study of very thin lubricant films in concentrated contacts. STLE Tribol Trans 1991;34:187–94.
[21] Guangteng G, Cann P, Olver AV, Spikes HA. Lubricant film thickness in rough surface, mixed elastohydrodynamic contact. J Tribol 2000;122:65–76.
[22] Cann PM, Spikes HA, Hutchinson J. The development of a spacer layer imaging method (SLIM) for mapping elastohydrodynamic contacts. Tribol Trans 1996;39:915–21.
[23] Gustafsson L, Hoglund E, Marklund O. Measuring lubricant film thickness with image analysis. Proc Inst Mech Eng: J, J Eng Tribol 1994;208:199–205.
[24] Hartl M, Krupka I, Liska M. Differential colorimetry: tool for evaluation of chromatic interference patterns. Opt Eng 1997;36(9):2384–91. http://dx.doi.org/10.1117/1.601415 URL: ⟨http://link.aip.org/link/?JOE/36/2384/1⟩.

[25] Greenwood JA, Kauzlarich JJ. Elastohydrodynamic film thickness for shear-thinning lubricants. Proc Inst Mech Eng, Part J: J Eng Tribol 1998;212 (3):179–91. http://dx.doi.org/10.1243/1350650981541994 arXiv:http://pij.sagepub.com/content/212/3/179.full.pdf+html, URL: ⟨http://pij.sagepub.com/content/212/3/179.abstract⟩.
[26] van Leeuwen H. The determination of the pressure—viscosity coefficient of a lubricant through an accurate film thickness formula and accurate film thickness measurements. Proc Inst Mech Eng, Part J: J Eng Tribol 2009;223 (8):1143–63. http://dx.doi.org/10.1243/13506501JET504 arXiv:http://pij.sagepub.com/content/223/8/1143.full.pdf+html, URL: ⟨http://pij.sagepub.com/content/223/8/1143.abstract⟩.
[27] Chittenden RJ, Dowson D, Dunn JF, Taylor MC. A theoretical analysis of the isothermal elastohydrodynamic lubrication of concentrated contacts. Part I. Direction of lubricant entrainment coincident with the major axis of the hertzian contact ellipse. Proc R Soc Lond Ser A 1985;397(1813):245–69.
[28] Hamrock BJ, Schmid SR, Jacobson B. Fundamentals of fluid film lubrication. 2nd ed. Basel: Dekker; 2004.
[29] Roelands C. Correlational aspects of the viscosity–temperature–pressure relationship of lubricating oils [Ph.D. thesis]. Delft University of Technology; 1967.
[30] Hamrock BJ, Dowson D. Ball Bearing Lubrication: The Elastohydrodynamics of Elliptical Contacts. New York: John Wiley & Sons; 1981. p. 386.
[31] Gupta PK, Cheng HS, Zhu D, Forster NH, Schrand JB. Viscoelastic effects in mil-l-7808-type lubricant. Part I. Analytical formulation. Tribol Trans 1992;35 (2):269–74. http://dx.doi.org/10.1080/10402009208982117 arXiv:http://www.tandfonline.com/doi/pdf/10.1080/10402009208982117, URL: ⟨http://www.tandfonline.com/doi/abs/10.1080/10402009208982117⟩.
[32] Gold PW, Schmidt A, Dicke , Loos J, Assmann C. Viscosity–pressure–temperature behavior of mineral and synthetic oils. J Synth Lubr 2001;18(1):51–79.
[33] Bair S, Gordon P. Rheological challenges and opportunities for ehl. In: Snidle R, Evans H. IUTAM symposium on elastohydrodynamics and micro-elastohydrodynamics, solid mechanics and its applications, vol. 134. Netherlands: Springer; 2006. p. 23–43.
[34] Krupka I, Bair S, Kumar P, Khonsari M, Hartl M. An experimental validation of the recently discovered scale effect in generalized Newtonian ehl. Tribol Lett 2009;33 (2):127–35. http://dx.doi.org/10.1007/s11249-008-9397-z URL: ⟨http://dx.doi.org/10.1007/s11249-008-9397-z⟩.
[35] Brandão JA, Meheux M, Seabra JHO, Ville F, Castro MJD. Traction curves and rheological parameters of fully formulated gear oils. Proc Inst Mech Eng, Part J: J Eng Tribol 2011;225:577–93, http://dx.doi.org/10.1177/1350650111405111.